

**Structural Determination of Molecular Overlayer Systems with Normal Photoelectron Diffraction:  $c(2 \times 2)$  CO-Ni(001) and  $(\sqrt{3} \times \sqrt{3})R30^\circ$  CO-Ni(111)**

S. D. Kevan,<sup>(a)</sup> R. F. Davis, D. H. Rosenblatt, J. G. Tobin,  
M. G. Mason,<sup>(b)</sup> and D. A. Shirley

*Materials and Molecular Research Division, Lawrence Berkeley Laboratory, Berkeley, California 94720,  
and Department of Chemistry, University of California, Berkeley, California 94720*

and

C. H. Li<sup>(c)</sup> and S. Y. Tong

*Department of Physics and Surface Studies Laboratory, University of Wisconsin-Milwaukee,  
Milwaukee, Wisconsin 53201*

(Received 28 April 1981)

Experimental and theoretical normal photoelectron diffraction studies of CO adsorbed on Ni are presented. It is shown for the first time that normal photoelectron diffraction can yield definitive structure determinations in molecular adsorbate systems. The linear-bonded atop geometry of  $c(2 \times 2)$  CO-Ni(001) is confirmed, while CO is found to occupy the twofold bridge site in  $(\sqrt{3} \times \sqrt{3})R30^\circ$  CO-Ni(111).

PACS numbers: 68.20.+t, 61.14.Fe, 79.60.Gs

The determination of molecular adsorbate bonding geometry is of major importance in surface science, but few structures are known to date. One popular experimental strategy combines photoemission, to establish the molecular species and orientation, with low-energy electron diffraction (LEED), for subsequent, quantitative structure studies. Recently it has been shown that normal photoelectron diffraction (NPD) alone is sufficient for structure determination in atomic overlayer systems.<sup>1,2</sup> In this Letter we report the first experimental evidence, for CO on two faces of nickel, that NPD can be used to determine *molecular* adsorbate structure. We chose to study  $c(2 \times 2)$ CO-Ni(001) because it has become a model molecular adsorption system and because LEED structure analysis has been difficult and the subject of controversy prior to the recent establishment of a generally accepted result.<sup>3</sup> In addition, we report the first accurate structure determination for the  $(\sqrt{3} \times \sqrt{3})R30^\circ$  CO-Ni(111) system, for which no LEED data presently exist. An NPD structural study has certain advantages relative to LEED. Radiation damage is minimal, long-range order is unnecessary, and the localized nature and phase coherence of NPD permits an independent structural determination for each atomic species in the molecule.

Experiments were performed on beam line I-1 at the Stanford Synchrotron Radiation Laboratory (SSRL) with an apparatus described elsewhere.<sup>4</sup> By using a grazing-incidence "grasshopper" monochromator equipped with a 1200-lines/mm holographic grating during dedicated operation,

we obtained photon flux and resolution sufficient to perform NPD experiments on both the C 1s and O 1s adsorbate core levels in the photon energy range  $300 \leq h\nu \leq 650$  eV. These experiments, together with our recent C 1s shape resonance measurements,<sup>5</sup> are the first systematic angle-resolved photoemission (ARP) studies of these light-element core levels with intermediate-energy x rays.

Clean and CO-covered nickel crystals were prepared and characterized with use of standard procedures.<sup>5</sup> LEED was not performed on the overlayer systems prior to NPD measurements, to avoid the usual primary-beam damage.<sup>3</sup> No time-dependent degradation of the overlayers (as determined by photoemission) was apparent over several hours of NPD experimentation. In addition, LEED measurements after the NPD studies confirmed the surface phases. This is a significant advantage of NPD in the study of molecular overlayers. Our  $(\sqrt{3} \times \sqrt{3})R30^\circ$  CO-Ni(111) sample yielded the very faint and diffuse LEED superstructure spots reported in the past for this system,<sup>6</sup> which have discouraged accurate LEED structure studies. However, NPD has been shown to be relatively insensitive to the degree of overlayer lateral order,<sup>1</sup> thus motivating its application to CO-Ni(111).

The NPD calculations were performed with use of a multiple-scattering algorithm detailed elsewhere.<sup>7,8</sup> All orders of multiple scattering were included. Carbon and oxygen phase shifts were generated with use of the  $X\alpha$  scattered-wave technique,<sup>7</sup> while those of nickel were derived

from the Wakoh self-consistent band-structure potential.<sup>9</sup> The inner potentials ( $V_0$ ) used were 11.2 and 10.5 eV for Ni(001) and Ni(111), respectively. The calculations were done for CO with the generally accepted orientation<sup>5</sup> (bond axis normal to the surface, with the carbon end down), in the top, bridge, and hollow sites, allowing the C-Ni interplanar distance ( $d_{\text{CNI}}^\perp$ ) and the CO bond distance ( $d_{\text{CO}}^\perp$ ) to vary in steps of 0.1 Å in a systematic search for the best fit to the experimental curves.

From the systematics of these calculations for the C 1s level in the CO-Ni(001) prototype system, we can draw important conclusions about the NPD process in *molecular* adsorbates. The theoretical results indicate<sup>8</sup> that if  $d_{\text{CO}}^\perp$  is held constant and  $d_{\text{CNI}}^\perp$  varied in successive calculations, the characteristic C 1s NPD modulation peak energy positions are shifted to higher kinetic energy as  $d_{\text{CNI}}^\perp$  is decreased, in agreement with the trend observed in earlier NPD studies of atomic overlayer systems.<sup>1</sup> In contrast, the peak positions do *not* disperse with  $d_{\text{CO}}^\perp$  in calculations where  $d_{\text{CNI}}^\perp$  is held constant. These observations imply that the C 1s experimental NPD curve should be extremely sensitive to  $d_{\text{CNI}}^\perp$ , but not to  $d_{\text{CO}}^\perp$ . This may be understood in terms of the localized nature of the NPD process. For the C 1s NPD curve to yield structural sensitivity to  $d_{\text{CO}}^\perp$ , the electron would have to undergo at least one scattering event off the oxygen atom. But the dominant scattering from oxygen is a small-angle forward scattering, and the phase difference between the scattered wave and the direct wave is essentially independent of the position of the oxygen atom, yielding little sensitivity to  $d_{\text{CO}}^\perp$ .<sup>8</sup> The situation is manifestly different for large-angle backscattering off nickel, which provides the sensitivity to  $d_{\text{CNI}}^\perp$ . Here, the backscattered wave accumulates phase in twice traversing the distance between absorbing and scattering atoms, so that substantial structural sensitivity is expected and observed.

The experimental NPD curve for the C 1s level, shown in the inset in Fig. 1, illustrates the above expectations. It represents the combined results of several experiments on different overlayer preparations and nickel crystals. Individually, peak positions were reproducible to  $\pm 1$ -2 eV from one experimental curve to another. As shown in the inset, the match between experimental and theoretical peak positions for  $d_{\text{CNI}}^\perp = 1.8$  Å and  $d_{\text{CO}}^\perp = 1.13$  Å in the atop geometry is excellent; peaks 1, 2, 3, and 4 fall at energies

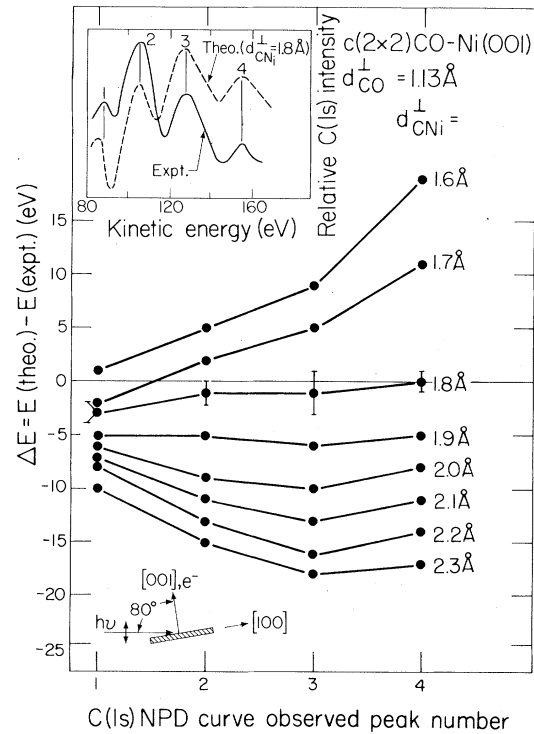


FIG. 1. Plot of  $\Delta E = E(\text{theor}) - E(\text{expt})$  vs NPD curve peak number for the C 1s level in  $c(2 \times 2)$  CO-Ni(001) with fixed CO bond length and various carbon-nickel spacings, with CO in the atop site. A comparison of calculated ( $d_{\text{CNI}}^\perp = 1.8$  Å,  $d_{\text{CO}}^\perp = 1.13$  Å) and experimental NPD curves is shown in the inset.

85, 105, 126, and 154 (theory) and 88, 106, 127, and 154 (experiment) eV kinetic energy, respectively. The quality of the experiment-theory fit can be examined quantitatively by observing the trend in  $\Delta E = E(\text{theor}) - E(\text{expt})$  for each of the four NPD peaks, as  $d_{\text{CNI}}^\perp$  is varied. These trends are summarized in Fig. 1. The criterion for a perfect match between theory and experiment,  $\Delta E = 0$  for each NPD peak, is most nearly met by the  $d_{\text{CNI}}^\perp = 1.8$  Å calculation. The systematic behavior shown in Fig. 1 simplifies the assessment of error limits for  $d_{\text{CNI}}^\perp$ . On the low side, which is more important for this case, the 1.7-Å curve is far outside the acceptable range. We adopt a very conservative lower limit of  $d_{\text{CNI}}^\perp = 1.76$  Å. On the high side, the longer distances shown are not credible for a C-Ni bond, on chemical grounds. However, even the 1.9 Å curve is off by several standard deviations. To raise it would require shifting the inner potential by  $\sim 5$  eV, from 11.2 to  $\sim 6$  eV, which is physically unacceptable. Our final adopted value is  $d_{\text{CNI}}^\perp = 1.80 \pm 0.04$  Å, with CO in the atop site.

From the above discussion it is clear that the O 1s NPD curve must be measured to determine  $d_{\text{CO}}^{\perp}$  from NPD alone. Theoretical and experimental results are summarized in Fig. 2. We were able to collect data over only the limited kinetic-energy range  $0 \leq E_k \leq 100$  eV because of poor photon flux and resolution above 400 eV. In general, measurement of C 1s and O 1s NPD intensities near  $E_k = 61$  eV was hampered by interference from the Ni  $M_{23}VV$  Auger peak<sup>1</sup> [see, e.g., dashed portion of experimental curve in Fig. 2(b)]. The theoretical curves [Fig. 2(a)] for fixed  $d_{\text{CNi}}^{\perp}$  and various CO illustrate that NPD structural results are less accurate in this lower-energy range because modulation peak position dispersion with  $d^{\perp}$  is lower, and additionally, the theoretical NPD curve shape is more model dependent for  $E_k \leq 60$  eV.<sup>1,8</sup> In spite of these limitations, a good fit of peak positions for  $d_{\text{CNi}}^{\perp} = 1.8$  Å and  $d_{\text{CO}}^{\perp} = 1.13$  Å is shown in Fig. 2(b). It is encouraging that the fit improves at higher energies. The NPD data show an excellent fit for the isolated molecule bond distance  $d_{\text{CO}}^{\perp} = 1.13$  Å, consistent with the LEED result of  $d_{\text{CO}}^{\perp} = 1.1$  Å,<sup>3</sup> but an O 1s study over a wider kinetic-energy range is desirable.

Figure 3 summarizes the extension of these CO-Ni studies to  $(\sqrt{3} \times \sqrt{3})R30^{\circ}$  CO-Ni(111). The C 1s NPD results shown in Fig. 3 confirm previous indications<sup>6</sup> that the CO adsorbate molecule is

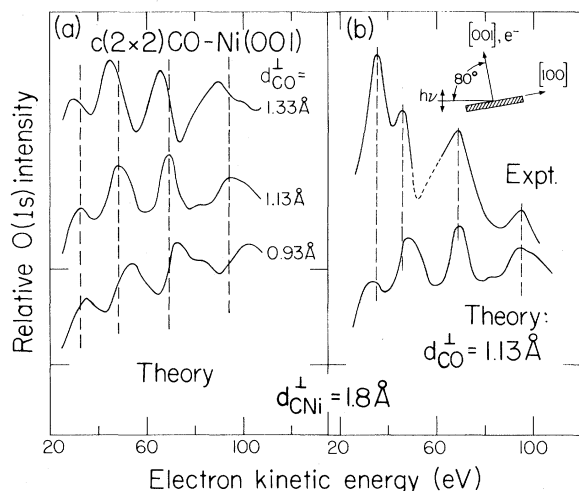


FIG. 2. (a) Calculated NPD curves for the O 1s level in  $c(2 \times 2)$  CO-Ni(001) for fixed carbon-nickel spacing and various CO bond lengths. (b) Comparison of the experimental result to the best-fit calculation from (a). The dashed portion of the experimental curve suffers from Ni  $M_{23}VV$  Auger interference.

bonded in the twofold bridge position on Ni(111). Aside from the region near  $E_k = 90$  eV, an excellent fit is obtained for  $d_{\text{CNi}}^{\perp} = 1.27 \pm 0.05$  Å in the bridge-bonded site, while poor fits are obtained for other values of  $d_{\text{CNi}}^{\perp}$  and other sites. Limited-energy-range O 1s results are also shown in Fig. 3. As with CO-Ni(001), the isolated molecule value of  $d_{\text{CO}}^{\perp} = 1.13$  Å gives the best agreement with theory. Again, because of the poor quality of the superstructure spots, a precise LEED analysis would have been impossible.

In conclusion, with use of normal photoelectron diffraction, the top-bonded CO structure for  $c(2 \times 2)$  CO-Ni(001) has been found, confirming recent detailed LEED investigations,<sup>3</sup> while the adsorbate is determined to occupy the twofold bridge site in  $(\sqrt{3} \times \sqrt{3})R30^{\circ}$  CO-Ni(111). Based on these observations and considerations discussed above, NPD shows promise for determining bonding geometries of molecular adsorbates, as a complementary or alternative method to LEED.

This work was supported by the Director, Office of Energy Research, Office of Basic Energy Sci-

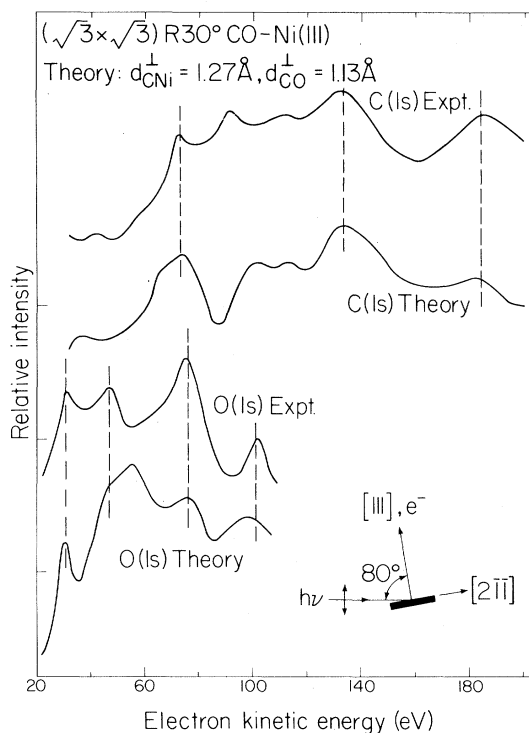


FIG. 3. Comparison of the best-fit calculation to experiment for both C 1s and O 1s levels in  $(\sqrt{3} \times \sqrt{3})R30^{\circ}$  CO-Ni(111). The calculations are for CO in the twofold bridge site.

ences, Chemical Sciences Division of the U. S. Department of Energy under Contract No. W-7405-ENG-48. It was performed in part at the Stanford Synchrotron Radiation Laboratory, which is supported by the National Science Foundation under Grant No. DMR-77-27489, in cooperation with the Stanford Linear Accelerator Center. We wish to acknowledge Mrs. Winifred Heppler for the preparation of the nickel crystals, and one of us (J. G. T.) would like to acknowledge a National Science Foundation graduate fellowship. This work was supported in part by National Science Foundation Grant No. DMR-77-28112 and by Petroleum Research Fund Grant No. 11584-AC5, 6.

<sup>(a)</sup>Permanent address: Bell Laboratories, Murray Hill, N.J. 07974.

<sup>(b)</sup>Permanent address: Research Laboratories, Eastman Kodak Company, Rochester, N.Y. 14650.

<sup>(c)</sup>Permanent address: Department of Physics, National Tsing Hua University, Hsinchu, Taiwan 300,

Republic of China.

<sup>1</sup>D. H. Rosenblatt, J. G. Tobin, M. G. Mason, R. F. Davis, S. D. Kevan, D. A. Shirley, C. H. Li, and S. Y. Tong, *Phys. Rev. B* **23**, 3828 (1981), and references therein.

<sup>2</sup>C. H. Li and S. Y. Tong, *Phys. Rev. Lett.* **42**, 901 (1979).

<sup>3</sup>S. Andersson and J. B. Pendry, *Surf. Sci.* **71**, 75 (1978), and *Phys. Rev. Lett.* **43**, 363 (1979); M. Passler, A. Ignatiev, F. Jona, D. W. Jepsen, and P. M. Marcus, *Phys. Rev. Lett.* **43**, 360 (1979).

<sup>4</sup>S. D. Kevan and D. A. Shirley, *Phys. Rev. B* **22**, 542 (1980).

<sup>5</sup>R. F. Davis, S. D. Kevan, D. H. Rosenblatt, M. G. Mason, J. G. Tobin, and D. A. Shirley, *Phys. Rev. Lett.* **45**, 1877 (1980), and references therein.

<sup>6</sup>J. C. Compuzano and R. G. Greenler, *J. Vac. Sci. Technol.* **16**, 445 (1979); W. Erley, H. Wagner, and H. Ibach, *Surf. Sci.* **80**, 612 (1979), and references therein.

<sup>7</sup>C. H. Li, A. R. Lubinsky, and S. Y. Tong, *Phys. Rev. B* **17**, 3128 (1978).

<sup>8</sup>C. H. Li and S. Y. Tong, *Phys. Rev. Lett.* **43**, 526 (1979).

<sup>9</sup>S. Wakoh, *J. Phys. Soc. Jpn.* **20**, 1896 (1965).

## Structure of Si(111)-(7×7)H

E. G. McRae and C. W. Caldwell<sup>(a)</sup>

*Bell Laboratories, Murray Hill, New Jersey 07974*  
(Received 26 November 1980)

Analysis of low-energy electron diffraction patterns for Si(111)-(7×7)H surface shows that they are consistent with a structural model of identical islands that are approximately triangular with  $[\bar{1}\bar{1}2]$  step boundaries and have area approximately half that of the 7×7 unit mesh and height within 5% of the bulk Si(111) double-layer spacing.

PACS numbers: 68.20.+t, 61.14.Hg

The nature of the (7×7)-fold periodic reconstruction of the annealed Si(111) surface is a long-standing question of fundamental importance for semiconductor surface physics.<sup>1</sup> In this paper we interpret low-energy electron-diffraction (LEED) evidence to show that the basic repeating unit of the 7×7 structure is an island of height equal to the Si(111) double-layer spacing. A model consisting of a 7×7 array of islands was suggested by Phillips.<sup>2</sup> Atomic-scattering data consistent with a double-layer island model were reported by Cardillo.<sup>3</sup> The present results not only provide experimental confirmation of the role of islands, but also indicate their size, shape, and lateral orientation as well.

Previous efforts to explain the 7×7 reconstruction have focused on the atomically clean surface Si(111)-(7×7). In principle, LEED data can be analyzed to determine the structure, but the exceedingly complicated LEED patterns obtained for the clean Si(111)-(7×7) surface have so far eluded even qualitative interpretation. However, we have been able to interpret the relatively simple LEED patterns that are observed for the H-covered surface Si(111)-(7×7)H (Fig. 1). The surface was obtained by exposing clean Si(111)-(7×7) to H atoms at room temperature as described by Sakurai and Hagstrum.<sup>4</sup>

Figure 1 illustrates the simplifying effect of H-atom adsorption on the LEED pattern. The effect